

Dimeric Complexes of a Tridentate Schiff Base Ligand – Crystal Structure of a Cu^{II} Complex with Uncommon μ_2 -N_{sulfonamido} Bridges and Ferromagnetic Behaviour

Jesús Sanmartín,^{*,[a]} Fernando Novio,^[a] Ana M. García-Deibe,^[b] Matilde Fondo,^[b] Noelia Ocampo,^[b] and Manuel R. Bermejo^[a]

Keywords: Sulfonamides / Schiff bases / N-donor ligands / Dimeric complexes / Ferromagnetism / Copper

N-[2-(Tosylamino)benzylidene]-2-[(tosylamino)methyl]aniline (H₂L) has afforded M^{II}₂(L)₂·xMeCN·yH₂O complexes (M = Ni, Pd, Cu, Zn and Cd; x = 0 or 2; y = 0, 4, 6 or 8). Physicochemical characterisation data are indicative of the dinuclear nature of the complexes obtained, where the potential N,N,N-donor L behaves as a dianionic and tridentate ligand. The crystal structure of Cu₂(L)₂·2MeCN was solved, and it demonstrates that a double μ_2 -N_{sulfonamido} bridge assembles the neutral Cu₂(L)₂ dimers. This uncommon connection gives

rise to a totally planar and nearly square-shaped Cu₂N₂ metallacycle. The planar geometries around the copper ions undergo a seesaw-shaped distortion, which is probably related to secondary Cu...O interactions with neighbouring tosyl groups. This spatial arrangement seems related to the ferromagnetic behaviour shown by the complex.

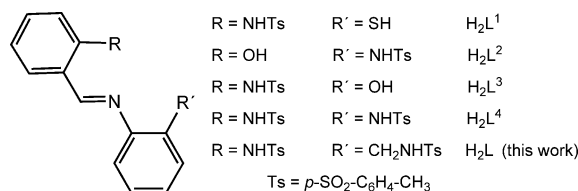
(© Wiley-VCH Verlag GmbH & Co. KGaA, 69451 Weinheim, Germany, 2008)

Introduction

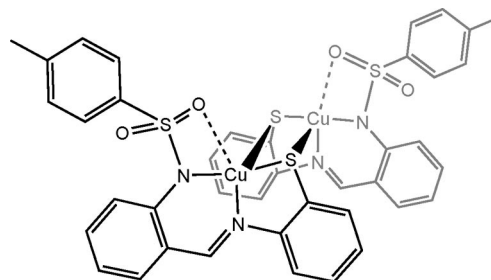
Research into physicochemical properties of complexes containing two or more metal centres in close proximity has received much attention.^[1–8] A common goal of many of these studies is a better understanding of the exchange interactions between paramagnetic centres, in order to correlate structural and magnetic properties.

Some dinuclear complexes with short M...M distances have been obtained from several tridentate tosylamino-functionalised Schiff base ligands depicted in Scheme 1.^[9–11] H₂L¹ has yielded Cu₂(L¹)₂,^[9] a complex with ferromagnetic behaviour, where both copper(II) ions are connected by two μ_2 -mercapto bridges (Scheme 2) and where the divalent copper ions display distorted tetragonal-pyramidal geometries, since an O atom of each tosyl group interacts with an adjacent metal centre. Furthermore, two pseudo-octahedral nickel(II) complexes, Ni₂(L²)₂(MeOH)₄·2MeCN^[10] and Ni₂(L³)₂(phen)₂,^[11] have also been reported (ligands shown in Scheme 1). In both cases, their cores are associated through double μ -phenoxido bridges. Likewise, undetermined bridges have also been proposed for dinuclear com-

plexes derived from H₂L⁴,^[12] however, only mononuclear nickel(II) and zinc(II) complexes, containing MeOH or 2-aminopyridine as coligands, have been crystallographically characterised.^[13]



Scheme 1. Some tosylamino-functionalised ligands mentioned in the text.



Scheme 2. Spatial arrangement for Cu₂(L¹)₂, with a “head-to-tail” π - π stacking interaction between conjugated blocks of the two Cu(L¹) units.

With the intention of synthesising some 3dⁿ and 4dⁿ dinuclear complexes ($n = 8–10$), we focused our studies on H₂L (Scheme 1). Although it seems to resemble H₂L⁴,^[12,13]

[a] Departamento de Química Inorgánica, Facultade de Química, Campus Sur, Universidade de Santiago de Compostela, 15782 Santiago de Compostela, Galicia, Spain
Fax: +34-981-597525
E-mail: qisuso@usc.es

[b] Departamento de Química Inorgánica, Facultade de Ciencias, Campus de Lugo, Universidade de Santiago de Compostela, 27002 Lugo, Spain

Supporting information for this article is available on the WWW under <http://www.eurjic.org> or from the author.

the presence of an additional methylene group in H_2L should favour the formation of the desired complexes. This expectation was based not only on an increase in flexibility, but on the improved donor ability of the $\text{N}_{\text{sulfonamido}}$ atom bonded to this methylene group, as we expected this group to partially balance the electron withdrawal caused by the neighbouring sulfonyl group.

Results and Discussion

Except for $\text{Pd}_2(\text{L})_2 \cdot 2\text{MeCN} \cdot 6\text{H}_2\text{O}$, which was obtained from $\text{Pd}(\text{AcO})_2$ by a chemical method described in the Experimental Section, the remaining complexes have been successfully prepared by oxidation of the corresponding sacrificial metal anode in an acetonitrile solution of H_2L . The simplicity, efficiency and cleanliness of this electrochemical method with the related ligands^[10–13] make this procedure a good alternative to traditional methods for the preparation of mono- and dinuclear neutral compounds, at least, with this type of ligands.

Microanalytical results are consistent with the presence of water and/or acetonitrile molecules in the formulae of these complexes. Water could come from acetonitrile, as this was used as purchased, without further purification, and under ambient conditions.

Since $\text{Ni}_2(\text{L})_2 \cdot 8\text{H}_2\text{O}$, $\text{Pd}_2(\text{L})_2 \cdot 2\text{MeCN} \cdot 6\text{H}_2\text{O}$ (see Supporting Information), $\text{Zn}_2(\text{L})_2 \cdot 4\text{H}_2\text{O}$ and $\text{Cd}_2(\text{L})_2 \cdot 6\text{H}_2\text{O}$ fragmentation patterns obtained from ESI^+ -MS analysis are very similar to those observed for $\text{Cu}_2(\text{L})_2 \cdot 2\text{MeCN}$, a dinuclear nature can be also deduced for these complexes.

Crystal Structure of $\text{Cu}_2(\text{L})_2 \cdot 2\text{MeCN}$

The asymmetric unit of $\text{Cu}_2(\text{L})_2 \cdot 2\text{MeCN}$ comprises a solvated acetonitrile molecule, which is disordered on two different sites (occupation: 60 and 40%), and half a molecule of the neutral complex $\text{Cu}_2(\text{L})_2$. This compound has been presented in Figure 1 as an ORTEP diagram, along with the labelling scheme used. Some representative geometric parameters have been listed in Table 1.

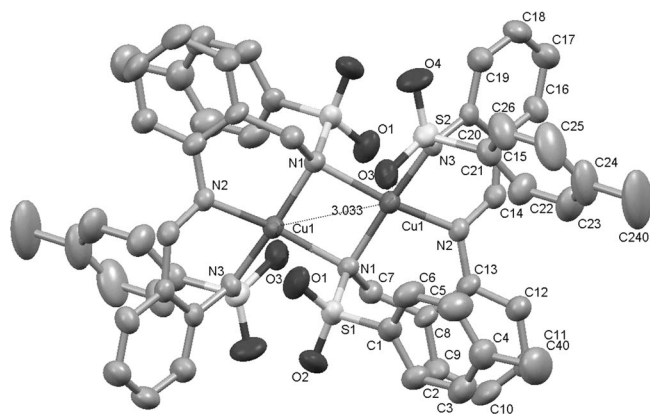


Figure 1. ORTEP view of the molecular structure of $\text{Cu}_2(\text{L})_2$, showing 40% probability displacement ellipsoids. H atoms have been omitted for clarity.

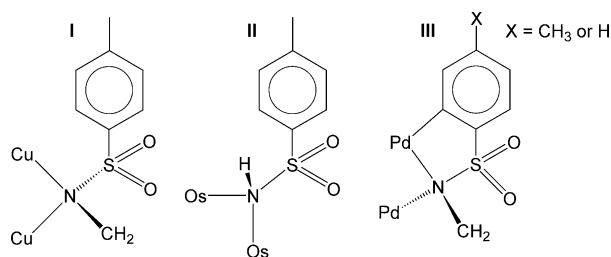
Table 1. Selected geometric parameters for $\text{Cu}_2(\text{L})_2 \cdot 2\text{MeCN}$ and H_2L .^[19]

Atoms ^[a]	Distance [Å]		Atoms ^[a]	Bond[°]	
	$\text{Cu}_2(\text{L})_2$	$\text{H}_2\text{L}^{[b]}$		$\text{Cu}_2(\text{L})_2$	$\text{H}_2\text{L}^{[b]}$
Cu1–N1	1.998(4)		N3–Cu1–N1	170.60(17)	
Cu1–N2	2.014(4)		N3–Cu1–N2	87.9(16)	
Cu1–N3	1.969(4)		N1–Cu1–N2	92.94(16)	
Cu1–N1 ^{#1}	2.118(4)		N3–Cu1–N1 ^{#1}	98.45(16)	
N1...N1 ^{#1}	2.785(4)		N1–Cu1–N1 ^{#1}	85.12(16)	
N1–C7	1.495(6)	1.476(3)	N2–Cu1–N1 ^{#1}	152.25(16)	
N1–S1	1.655(4)	1.616(2)	Cu1–N1–Cu1 ^{#1}	94.88(18)	
S1–O1	1.445(4)	1.429(3)	C1–S1–N1	110.2(2)	107.4(2)
S1–O2	1.441(4)	1.431(3)	C7–N1–S1	113.4(3)	119.3(2)
N2–C13	1.428(6)	1.416(3)	O1–S1–O2	118.7(3)	119.7(2)
N2–C14	1.292(6)	1.277(3)	N2–C14–C15	128.1(5)	123.9(2)
N3–C20	1.380(6)	1.403(3)	C13–N2–C14	116.7(4)	120.5(2)
N3–S2	1.614(4)	1.620(3)	C20–N3–S2	120.2(4)	127.6(2)
S2–O3	1.441(4)	1.432(2)	N3–S2–C21	105.8(2)	106.1(2)
S2–O4	1.441(4)	1.432(2)	O3–S2–O4	115.6(2)	119.6(2)

Atoms	Torsion [°]	
	$\text{Cu}_2(\text{L})_2$	$\text{H}_2\text{L}^{[c]}$
S1–N1–C7–C8	69.0(5)	–122.23(18); –135.79(16); –128.96(18)
N1–C7–C8–C13	55.9(7)	–100.5(2); –71.7(2); –70.7(3)
C7–C8–C13–N2	1.8(7)	2.0(3); –1.5(3); 6.1(3)
C13–N2–C14–C15	171.7(5)	–176.30(18); 172.5(2); 174.74(19)
C15–C20–N3–S2	–141.5(4)	168.22(18); 170.69(17); 152.43(19)
C20–N3–S2–C21	61.9(4)	72.1(2); –67.2(2); –54.1(2)

[a] Symmetry transformations used to generate equivalent atoms: ^{#1} $-x, -y + 1 - z + 1$. [b] Average value found for three different polymorphs solved for H_2L .^[19] [c] Values of the corresponding torsion for each one of the three polymorphs solved for H_2L .^[19]

This dimeric complex results from the pairing of two neutral $\text{Cu}(\text{L})$ units, with an inversion centre (^{#1} $-x, -y + 1, -z + 1$) at the centre of the molecule. These units are assembled by means of two slightly asymmetric μ_2 - $\text{N}_{\text{sulfonamido}}$ bridges that give rise to a completely planar and nearly square-shaped Cu_2N_2 metallacycle (Table 1 and Figure 1). A search in the Cambridge Structural Database^[14] indicates that the μ_2 -N connections found in $\text{Cu}_2(\text{L})_2 \cdot 2\text{MeCN}$ (Scheme 3a) could be considered as novel for sulfonamido ligands.



Scheme 3. Bridging coordination modes that include a μ_2 - $\text{N}_{\text{sulfonamido}}$ connection found for arylsulfonamide residues: (a) $\text{Cu}_2(\text{L})_2 \cdot 2\text{MeCN}$;^[14] (b) $(\mu_2\text{-H})(\mu_2\text{-NHTs})\text{Os}_3(\text{CO})_{10}$;^[15] (c) μ_2 - η^2 : η^1 -N,C² chelating behaviour of two *N*-(arylsulfonyl)glycinato ligands.^[18]

With regard to this novelty, although a μ_2 -NHTs bridge (Ts = *p*-tolylsulfonyl) has been reported for $(\mu_2\text{-H})(\mu_2\text{-NHTs})\text{Os}_3(\text{CO})_{10}$ (Scheme 3b),^[15] the sulfonamide nature of this bridging ligand may be questionable. In fact, the tosylamine H atom of this bridge was inserted in its theoretical idealised position. This strongly contrasts with all the remaining H atoms of this compound, which were located in difference Fourier maps. In addition, geometric data corresponding to this sulfonamido bridge are reminiscent of other μ_2 -N bridges that have been subsequently described as either sulfonylimido or sulfonylnitrene connections.^[16] This difference is not trivial, if we consider their greater ability for electron donation in comparison with a sulfonamide group. In fact, many complexes containing sulfonylimido or sulfonylnitrene μ_2 -N,^[16] and even μ_3 -N, links^[17] have been reported.

Two interesting tetranuclear cyclometallated palladium(II) complexes^[18] present some similarities to $\text{Cu}_2(\text{L})_2 \cdot 2\text{MeCN}$, as they also show a coordination mode including $\mu_2\text{-N}_{\text{sulfonamido}}$ bridges through their arylsulfonyl residues. However, their *ortho* C_{aryl} atoms are further coordinated to one of the metal centres, and in consequence, this coordination mode must be described as $\mu_2\text{-}\eta^2\text{:}\eta^1\text{-N,C}^2$ (Scheme 3c). In our opinion, the presence of a methylene group adjacent to their $\mu_2\text{-N}_{\text{sulfonamido}}$ bridges, as occurs in $\text{Cu}_2(\text{L})_2$, could be a significant feature of these dimeric Pd^{II} complexes, as opposed to a mere coincidence.

The unusual μ_2 -N coordination mode found in $\text{Cu}_2(\text{L})_2$ clearly entails an sp^3 hybridisation of the bridging N atom. This strongly contrasts with typical sp^2 geometries displayed not only by the sulfonamide S atoms of the free ligand (Table 1),^[19] but also by those of many other sulfonamido ligands, both free^[13,18,20b–20d] and η^1 -coordinated.^[9–13,18,20,21] This divergence can be easily perceived in Figure 2, as L^{2-} displays both coordination modes: bridging μ_2 -N (N1), and terminal η^1 -N (N3), with sp^3 and sp^2 geometries, respectively.

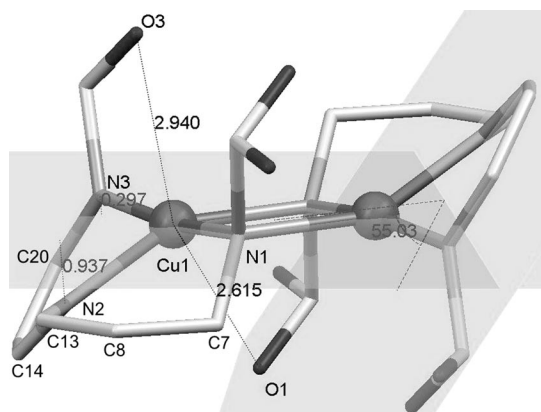


Figure 2. Ball-and-stick representation of the core of $\text{Cu}_2(\text{L})_2$, including SO_2 groups and chelate rings. Secondary interactions with tosyl O atoms, as well as distances from N_{imine} and terminal $\text{N}_{\text{sulfonamido}}$ donor atoms to the metallacyclic plane have been also indicated.

The change of hybridisation caused by the bridging coordination of N1 clearly affects the conformation of the N1–C7 bonds. Thus, a comparison between Newman projections of this bond for $\text{Cu}_2(\text{L})_2$ and the three polymorphs (**T_a**, **T_c** and **M**) reported for $\text{H}_2\text{L}^{[19]}$ (Figure 3) shows that S1 and C8 are nearly *anti* positioned and eclipsed in the free ligand, whereas the two atoms clearly have the *gauche* conformation in $\text{Cu}_2(\text{L})_2 \cdot 2\text{MeCN}$.

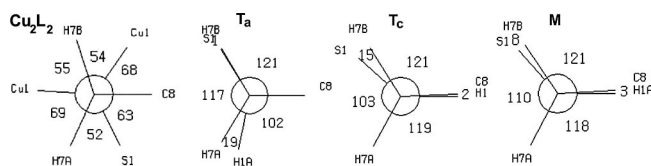


Figure 3. Newman projections of the N1–C7 bonds for $\text{Cu}_2(\text{L})_2 \cdot 2\text{MeCN}$ and three conformers of the free ligand (**T_a**, **T_c** and **M**).^[19]

Coordination environments around the copper(II) ions can be considered as distorted square-planar, according to their geometric parameters (Table 1). Their distortion can be described as seesaw-shaped, since only the imine N atoms (N2) visibly protrude from the plane containing the Cu_2N_2 metallacycle (Figure 2). Cu–N distances are within usual ranges reported for other copper(II) complexes with related ligands.^[9,10,20] In addition, typical interactions with adjacent O atoms of the tosyl groups^[9–13,18,20,21] can be detected (Figure 2), but they seem too long to be considered as true coordination bonds.

These contacts between tosyl groups and copper(II) ions may favour the evident torsion suffered by the conjugated block of the ligand in the complex (Figure 2 and Figure 4). In fact, least-squares-calculated planes for those aromatic rings corresponding to the diamine (C8–C13) and the aldehyde (C15–C20) residues form an angle of ca. 59.2° . This loss of coplanarity could be also favoured by the coordination of the imine N2 atom, which, in accordance with data collected in Table 1, appears to weaken the double character of the C14=N2 bond slightly.

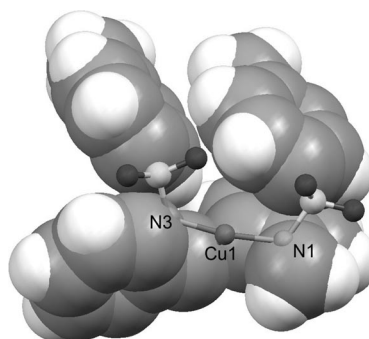


Figure 4. Representation of one of the $\text{Cu}(\text{L})$ units in $\text{Cu}_2(\text{L})_2 \cdot 2\text{MeCN}$. C and H atoms have been represented as space-filling objects to show both the orientation and the stacking of the aromatic groups. Cu, N and O atoms are represented as ball-and-stick models to show the ability and predisposition of N1 to act as a bridge.

The flexibility afforded by the methylene group allows the formation of wide angles between the two chelate planes of the same ligand (about 42°), as well as between the planar Cu_2N_2 metallacycle and the chelate plane calculated for the aldehyde residue (Figure 2). Likewise, it could also be related to the marked backward bending observed for both tosyl groups in $\text{Cu}_2(\text{L})_2 \cdot 2\text{MeCN}$, which leads to intra-ligand π - π interactions (Figure 1 and Figure 4) and allows a “frontal” interaction of two inverted $\text{Cu}(\text{L})$ units (Figure 4) through N1, which is able to form μ_2 -N_{sulfonamido} bridges.

Both intermolecular π - π and $\text{C}-\text{H} \cdots \text{O}$ contacts seem to be the base of a crystal packing scheme lacking significant $\text{C}-\text{H} \cdots \pi$ contacts and including several intramolecular $\text{C}-\text{H} \cdots \text{O}$ interactions. Some of these latter interactions seem similar to those found for H_2L ^[19] (Supporting Information).

EPR and Magnetic Susceptibility Studies

X-band EPR powder spectra have been recorded for a polycrystalline sample of $\text{Cu}_2(\text{L})_2 \cdot 2\text{MeCN}$ in the range 8–300 K. These spectra show a single broad-band resonance at $g_{\text{iso}} \approx 2.13$ (Figure 5, top) that corresponds to the allowed

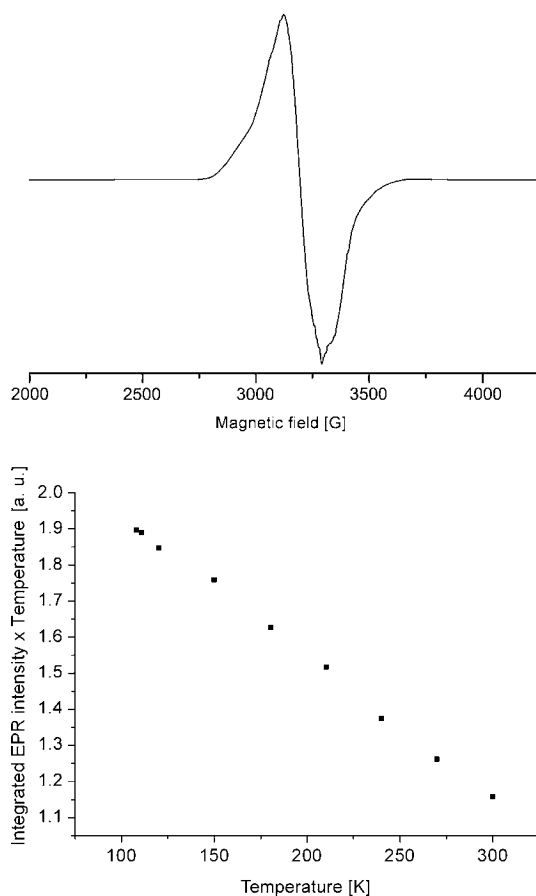


Figure 5. X-band (9.45 GHz) powder spectrum at 9 K (top) and temperature behaviour in the range 300–108 K of the product of integrated EPR intensity and temperature (bottom) for $\text{Cu}_2(\text{L})_2 \cdot 2\text{MeCN}$.

$\Delta M_S = 1$ transition.^[22] The increase in the integrated EPR intensity with decreasing temperature (Figure 5, bottom) shows a tendency similar to that reported for a ferromagnetic dimeric copper(II) complex containing *N,N*-diisopropylthiocarbamate,^[23] which suggests a ferromagnetic coupling of the copper ions in $\text{Cu}_2(\text{L})_2 \cdot 2\text{MeCN}$. The variation of the signal intensity with temperature could be interpreted as a thermal depopulation as temperature decreases from a higher energy state to the ground one. To illustrate this, Figure 5 (bottom) shows the correlation between temperature and the product of integrated intensity and temperature. This eliminates the intrinsic temperature dependence of the EPR signal caused by the Boltzmann population of the Zeeman levels involved.

The magnetic behaviour of $\text{Cu}_2(\text{L})_2 \cdot 2\text{MeCN}$ has been investigated in the 2–300 K temperature range, and a plot of $\chi_M T$ vs. T is shown in Figure 6. The $\chi_M T$ value at 300 K ($0.90 \text{ cm}^3 \text{ mol}^{-1} \text{ K}$) is slightly higher than $0.85 \text{ cm}^3 \text{ mol}^{-1} \text{ K}$, the value expected for two uncoupled copper(II) ions with $g = 2.13$, as deduced from the EPR spectra. This value increases upon cooling to reach a maximum at about 20 K ($1.09 \text{ cm}^3 \text{ mol}^{-1} \text{ K}$) and then decreases with diminishing temperature. This behaviour suggests a ferromagnetic interaction between the Cu^{II} ions. The quick diminution in $\chi_M T$ at low temperatures can be attributed to interdimeric anti-ferromagnetic interactions and/or to the zero-field-splitting effect of the $S = 1$ ground state. The experimental data were fitted to the Bleaney–Bowers equation [Equation (1)]^[24] modified for intermolecular interactions according to the crystal structure of $\text{Cu}_2(\text{L})_2$.

$$\chi_M T = \frac{Ng^2\beta^2TF(J,T)}{kT - J'F(J,T)} \quad (1)$$

$$\text{with} \quad F(J,T) = \frac{2}{3 + \exp(-J/kT)}$$

The spin Hamiltonian used is $H = -JS_1S_2$, and the symbols in this equation have their usual meaning.

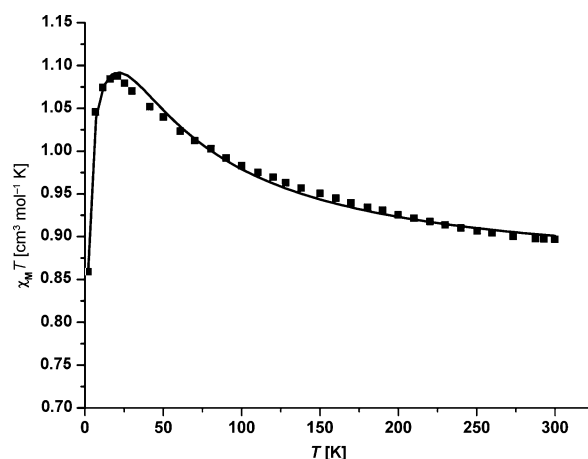


Figure 6. A plot of $\chi_M T$ vs. T for $\text{Cu}_2(\text{L})_2 \cdot 2\text{MeCN}$. Scattered points are the experimental results, and the solid line represents the best fit.

The fitting was performed by fixing the g value to that obtained from EPR measurements, which is 2.13. The best least-squares fit (Figure 6) gave the following parameters: $J = 54.4 \text{ cm}^{-1}$, and $J' = -0.66 \text{ cm}^{-1}$ ($R = 4.0 \times 10^{-5}$). Attempts were made to compare this J value with those reported in literature. Nevertheless, to the best of our knowledge, no crystallographically characterised dinuclear copper complexes with μ_2 -N_{sulfonamido} bridges have been previously magnetically analysed. However, several experimental and theoretical studies of azido-bridged complexes containing a Cu_2N_2 core have been performed, and some magneto-structural correlations seem to emerge from these studies.^[25] For instance, in these compounds, ferromagnetic coupling is expected when the Cu–N–Cu angles are less than 108° , and the positive J value increases as the angle decreases, though the correlation is not linear.

In our case study, the crystal structure of $\text{Cu}_2(\text{L})_2 \cdot 2\text{MeCN}$ shows that the copper atoms are in square-planar environments in which both $d_{x^2-y^2}$ magnetic orbitals point to the bridging N atoms. Therefore, the magnetic exchange pathway is a double μ_2 -N bridge too. Furthermore, it could be worth mentioning that the Cu_2N_2 core is absolutely planar, without roof-shaped distortion. Hence, despite the sp^3 character of the bridging N atom orbitals, the superexchange mechanism in our compound could be considered to be similar to that displayed in doubly bridged end-on

azido complexes.^[25] Accordingly, taking into account that the Cu–N–Cu angle in $\text{Cu}_2(\text{L})_2$ is about 94.9° , an intramolecular ferromagnetic coupling could be anticipated, in good agreement with the experimental results.

This ferromagnetic behaviour could be also predicted from the energy gap between the frontier molecular orbitals. Thus, extended Hückel calculations have been carried out, by means of the CACAO program,^[26] with the crystallographic coordinates of $\text{Cu}_2(\text{L})_2 \cdot 2\text{MeCN}$, taking into account the whole $\text{Cu}_2(\text{L})_2$ complex and excluding the atomic coordinates of the solvated MeCN molecules. This computation shows that the HOMO and LUMO orbitals (Figure 7) result from the combination of the $d_{x^2-y^2} \pm d_{x^2-y^2}$ couple with p orbitals of the N-bridging atoms (N1) and ter-

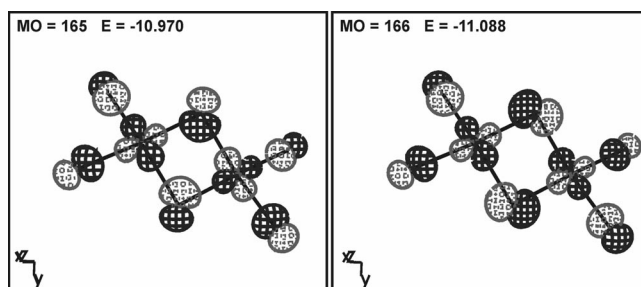


Figure 7. Frontier molecular orbitals for $\text{Cu}_2(\text{L})_2$.

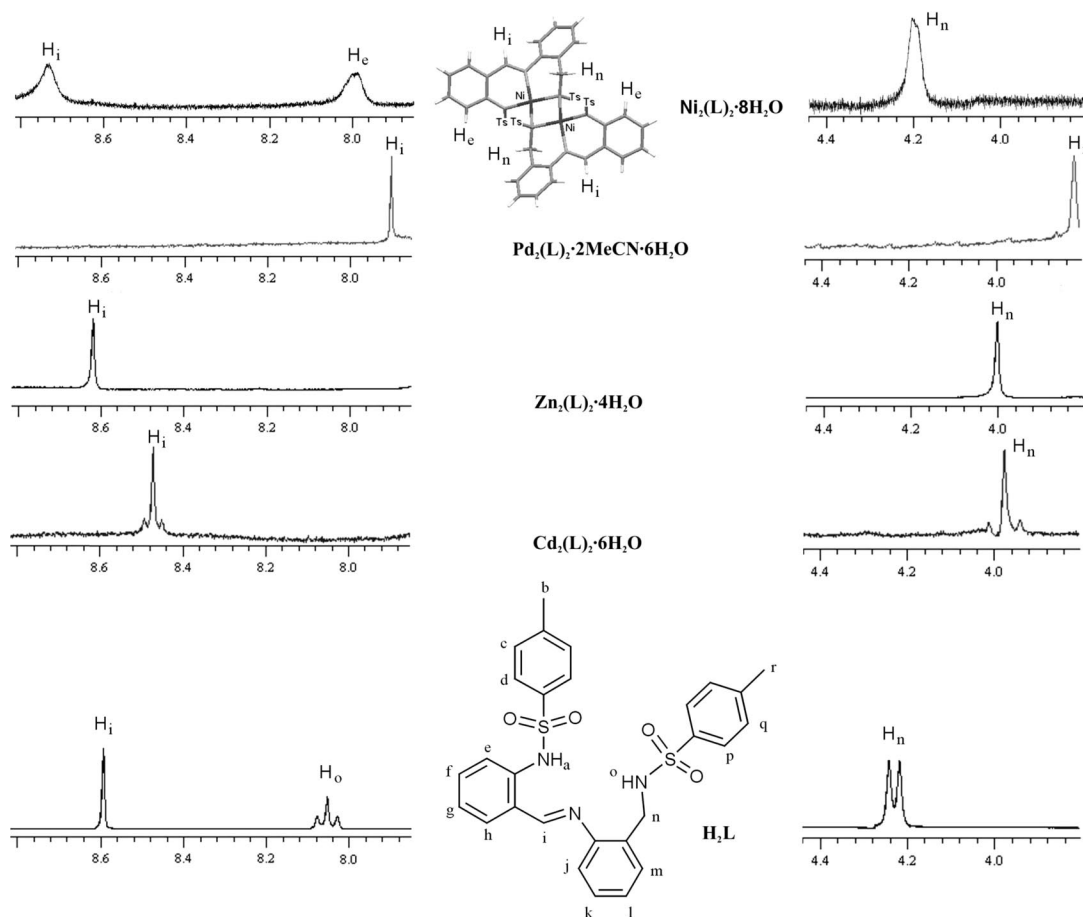


Figure 8. View of azomethine (left) and methylene (right) proton signals in the ^1H NMR spectra of the free ligand^[19] and their complexes in $[\text{D}_6]\text{dmso}$.

minal donors (N2 and N3), as expected. In addition, these calculations estimate a small HOMO–LUMO gap of about 0.118 eV. Although the CACAO program does not give accurate quantitative energy values, it can be used as a good qualitative guide. Hence, the small energetic HOMO–LUMO gap observed in this case could reasonably give rise to a parallel alignment of the unpaired electrons;^[8,27–28] and therefore, this result also seems to support the experimental magnetic data.

NMR Spectroscopic Studies

The diamagnetism of the palladium(II) and nickel(II) complexes provides evidence for an electronic pairing in the d_{xz} , d_{yz} , d_{z^2} and d_{xy} orbitals, which is coherent with the square-planar geometries of these d^8 ions.

The disappearance of both sulfonamido protons present at 12.16 ppm (s, 1 H, H_a) and 8.05 ppm (t, $J = 6.0$, 6.2 Hz, 1 H, H_o) in the free ligand spectrum^[19] as well as variable shifts affecting the signals corresponding to the azomethine, methylene and even aromatic protons (Figure 8) reveal the bideprotonation and complexation of H_2L in forming these metal complexes.

Regarding the behaviour of the methylene group, H_n signals observed for the Ni^{II} , Pd^{II} , Zn^{II} and Cd^{II} complexes are appreciably different from that for the free ligand [$\delta = 4.23$ ppm (d, $J = 6.2$ Hz, 2 H)]^[19] (Figure 8). The multiplicity changes from a doublet to a singlet as a result of the disappearance of the H_n – H_o coupling. In addition, this signal undergoes a slight upfield shift, which becomes especially evident in the spectrum of the palladium(II) complex (0.41 ppm). The observation of only one signal for the two methylene protons, both in the spectra of the free ligand (as a doublet) and in those corresponding to their complexes (as singlets), should be a consequence of an enantiotopic rather than a diastereotopic nature of these geminal protons on the NMR timescale.^[29]

Conclusions

The designed N,N,N-donor Schiff base ligand seems suitable for yielding dimeric Ni^{II} , Pd^{II} , Cu^{II} , Zn^{II} and Cd^{II} complexes through μ_2 - $N_{\text{sulfonamido}}$ bridges. The electrochemical method employed in the synthesis of the complexes is a good alternative to a classical chemical approach in this case. The presence of a methylene group adjacent to one of the sulfonamide groups could be related to the change from a typical sp^2 to a sp^3 hybridisation of the neighbouring $N_{\text{sulfonamido}}$ atom.

$Cu_2(L)_2 \cdot 2MeCN$ results from the coupling of two mononuclear $Cu(L)$ units through a double μ_2 - N connection that gives rise to a totally planar and nearly square-shaped Cu_2N_2 metallacycle. The $N_{\text{sulfonamido}}$ atoms seem to mediate a ferromagnetic coupling, which can be satisfactorily explained in terms of the acute Cu–N–Cu angles observed and the small energetic HOMO–LUMO gap.

Experimental Section

Materials and Methods: Chemicals of the highest commercial grade available (Aldrich) were used as received, without further purification. Elemental analyses were performed with a Carlo Erba EA 1108 analyser. Positive electrospray ionisation mass spectra were recorded with a LC/MSD Hewlett Packard 1100 spectrometer, by using methanol as solvent (2% formic acid). The samples had been previously dissolved in the minimum amount of dimethyl sulfoxide. NMR spectra were recorded with Bruker spectrometers, by using $[D_6]dmsO$ as solvent. Infrared spectra were recorded by using KBr pellets with a Bio-Rad FTS 135 spectrophotometer in the range 4000–600 cm^{-1} . The diffuse reflectance spectrum was recorded with a Shimadzu UV-3101 PC spectrophotometer. Magnetic susceptibilities were measured by using a SQUID magnetometer. Diamagnetic corrections were made by use of Pascal's constants. Powder EPR spectra were obtained by using a Varian E-109 spectrometer equipped with a rectangular resonant cavity and 100 kHz field modulation and an ITC503 Oxford cryogenic system to vary the temperature. A HP5352B frequency counter was used to measure the microwave frequency. The EPR spectra were acquired and digitised by a microcomputer equipped with a standard data acquisition card with an analogue-to-digital converter. These characterisation analyses were performed by in-house services (CACTUS).

Ligand Synthesis: H_2L was obtained by a classical Schiff condensation of 2-(tosylamino)benzaldehyde and 2-[(tosylamino)methyl]aniline.^[19] The latter compound resulted from the selective tosylation of (2-aminobenzyl)amine.

Synthesis of the Complexes: $Pd_2(L)_2 \cdot 2MeCN \cdot 6H_2O$ was obtained by heating under reflux over a 6-h period a methanol solution containing H_2L , NaOH and $Pd(AcO)_2$ in a 1:2:1 molar ratio. Filtration of the resulting suspension yielded a solid, which was washed with diethyl ether and dried in vacuo. The endpoint of this reaction was determined by TLC.

The remaining complexes have been obtained by an electrochemical method, in which a sacrificial metal anode was oxidised in an acetonitrile solution of H_2L . The cells can be summarised as: $M_{(+)}|H_2L_{(MeCN)} + NMe_4ClO_{4(MeCN)}|Pt_{(-)}$. (**Caution:** Although no problem has been encountered in this work, all perchlorate compounds are potentially explosive and should be handled in small quantities and with great care!) The preparation of $Cu_2(L)_2 \cdot 2MeCN$ is outlined below.

An acetonitrile solution (75 cm^3) of H_2L (100 mg, 0.187 mmol), containing tetraethylammonium perchlorate (ca. 20 mg), was electrolysed for 2 h at a current intensity of 5 mA and an initial voltage of 8 V. A slow and partial evaporation of the resulting solution yielded greenish-brown crystals of $Cu_2(L)_2 \cdot 2MeCN$ suitable for X-ray studies. A faster concentration in vacuo until saturation yielded a brown raw product that was characterised as $Cu_2(L)_2 \cdot 2MeCN \cdot 8H_2O$, even after being washed with diethyl ether and dried in vacuo, but whose characterisation data are similar to those of $Cu_2(L)_2 \cdot 2MeCN$.

$Ni_2(L)_2 \cdot 8H_2O$: Green powder. Yield 0.37 g (77%); m.p. 265 °C. $C_{56}H_{50}N_6Ni_2O_8S_4 \cdot 8H_2O$ (1324.7): calcd. C 50.77, H 5.02, N 6.34, S 9.68; found C 50.95, H 5.42, N 6.94, S 9.37. ESI⁺-MS (15 V): m/z (%) = 1181.0 (45) $[Ni_2(L)_2]^+$, 1145.1 (100) $[Ni(HL)_2 + Na]^+$. FTIR (KBr): $\tilde{\nu} = 3443$ (b, s) $\nu(O-H)$, 1607 (s) $\nu(C=N)$, 1305 (sh) $\nu(C-N)$, 1267 (s) $\nu_{as}(SO_2)$, 1161 (s) $\nu_s(SO_2)$ cm^{-1} . 1H NMR (400 MHz, $[D_6]dmsO$): $\delta = 8.74$ (s, 1 H, HC=N), 8.0–7.0 (m, 16 H, H_{arom}), 4.20 (s, 2 H, H_2C), 2.31 (s, 3 H, H_3C), 2.30 (s, 3 H, H_3C) ppm.

Pd₂(L)₂·2MeCN·6H₂O: Brown powder. Yield 0.24 g (82%); m.p. 250 °C. C₅₆H₅₀N₆O₈Pd₂S₄·2MeCN·6H₂O (1464.8): calcd. C 49.15, H 4.64, N 7.65, S 8.74; found C 49.60, H 4.25, N 7.31, S 7.55. ESI⁺-MS (150 V, see Supporting Information): *m/z* (%) = 1298.8 (100) [Pd₂(L)₂ + Na]⁺, 1193.0 (72) [Pd(HL)₂ + Na]⁺. FTIR (KBr): $\tilde{\nu}$ = 3340 (b, m) ν (O–H), 1580 (vs) ν (C=N), 1333 (m) ν (C–N), 1277 (s) $\nu_{\text{as}}(\text{SO}_2)$, 1116 (s) $\nu_{\text{s}}(\text{SO}_2)$, 672 (m) ν (C–S) cm^{−1}. ¹H NMR (300 MHz, [D₆]dmsO): δ = 7.90 (s, 1 H, HC=N), 7.75–6.90 (m, 16 H, H_{arom}), 3.82 (s, 2 H, H₂C), 2.34 (s, 3 H, H₃C), 2.32 (s, 3 H, H₃C) ppm.

Cu₂(L)₂·2MeCN: Greenish-brown crystals. Yield 0.17 g (72%); m.p. 235 °C. C₅₆H₅₀Cu₂N₆O₈S₄·2MeCN (1272.45): calcd. C 56.58, H 4.40, N 8.80, S 10.06; found C 56.45, H 4.59, N 8.74, S 9.88. ESI⁺-MS (125 V): *m/z* (%) = 1212.8 (100) [Cu₂(L)₂ + Na]⁺, 1190.9 (52) [Cu₂(L)₂ + H]⁺, 1152.0 (33) [Cu(HL)₂ + Na]⁺. FTIR (KBr): $\tilde{\nu}$ = 3443 (b, s) ν (O–H), 1604 (s) ν (C=N), 1265 (s) $\nu_{\text{asym}}(\text{SO}_2)$, 1129 (s) $\nu_{\text{sym}}(\text{SO}_2)$ cm^{−1}. UV/Vis: λ = 630 (d_{xy} → d_{x²−y²}) nm.

Zn₂(L)₂·4H₂O: Yellow powder. Yield 0.16 g (69%); m.p. 295 °C. C₅₆H₅₀N₆O₈S₄Zn₂·4H₂O (1264.8): calcd. C 53.13, H 4.59, N 6.64, S 10.12; found C 53.27, H 4.98, N 6.84, S 9.42. ESI⁺-MS (15 V): *m/z* (%) = 1194.8 (100) [Zn₂(L)₂ + H]⁺, 1131.0 (59) [Zn(HL)₂ + H]⁺. FTIR (KBr): $\tilde{\nu}$ = 3436 (b, m) ν (O–H), 1612 (vs) ν (C=N), 1328 (m) ν (C–N), 1265 (s) $\nu_{\text{as}}(\text{SO}_2)$, 1132 (s) $\nu_{\text{s}}(\text{SO}_2)$, 665 (s) ν (C–S) cm^{−1}. ¹H NMR (300 MHz, [D₆]dmsO): δ = 8.61 (s, 1 H, HC=N), 7.80–6.92 (m, 16 H, H_{arom}), 3.99 (s, 2 H, H₂C), 2.33 (s, 3 H, H₃C), 2.31 (s, 3 H, H₃C) ppm. ¹³C NMR (125 MHz, [D₆]dmsO): δ = 169.0 (1 C, HC=N), 137.5–118.0 (24 C, 24C_{arom}), 48.5 (1 C, H₂C), 21.1 (2 C, CH₃) ppm.

Cd₂(L)₂·6H₂O: Yellow powder. Yield 0.20 g (75%); m.p. 280 °C. C₅₆H₅₀Cd₂N₆O₈S₄·6H₂O (1394.8): calcd. C 48.18, H 4.45, N 6.02, S 9.18; found C 47.96, H 4.30, N 5.92, S 8.47. ESI⁺-MS (10 V): *m/z* (%) = 1290.0 (12) [Cd₂(L)₂ + H]⁺. FTIR (KBr): $\tilde{\nu}$ = 3441 (b, m) ν (O–H), 1595 (vs) ν (C=N), 1291 (m) $\nu_{\text{as}}(\text{SO}_2)$, 1160 (s) $\nu_{\text{s}}(\text{SO}_2)$, 663 (m) ν (C–S) cm^{−1}. ¹H NMR (300 MHz, [D₆]dmsO): δ = 8.45 (s, 1 H, HC=N), 7.80–6.90 (m, 16 H, H_{arom}), 3.98 (s, 2 H, H₂C), 2.29 (s, 3 H, H₃C), 2.27 (s, 3 H, H₃C) ppm.

Crystallographic Data for Cu₂(L)₂·2MeCN: C₆₀H₅₆Cu₂N₈O₈S₄, *M_w* = 1272.45, crystal system: triclinic, crystal group: *P* $\bar{1}$ (No. 2), *a* = 11.1244(12) Å, *b* = 11.1921(18) Å, *c* = 13.470(2) Å, α = 66.498(12)°, β = 80.812(11)°, γ = 70.504(1)°, *V* = 1449.1(4) Å³, *Z* = 1; *D*_{calcd.} = 1.458 g cm^{−3}; μ (Cu-*K* α) = 2.765 mm^{−1}; 6073 refl. measured, 5760 refl. unique (*R*_{int} = 0.0852). The diffraction data were collected at 293(2) °C with an Enraf Nonius Turbo CAD4 diffractometer, (Cu-*K* α graphite-monochromatised radiation λ = 1.54184 Å, $2\theta_{\text{max}}$ = 72.97). Data were processed and corrected for decay (55%), as well as for Lorentz, polarisation and absorption (psi-scan) effects. The structure was solved by direct methods and refined by full-matrix least-squares based on *F*², by using SHELX-97 software,^[30] giving final *R*₁ = 0.0577, *wR*₂ = 0.1413 [*I* > 2σ(*I*)]; *R*₁ = 0.1713, *wR*₂ = 0.1790 (all data). All non-hydrogen atoms were anisotropically refined, except those corresponding to disordered solvated MeCN molecules, which were isotropically treated. Hydrogen atoms were included in the model at geometrically calculated positions and refined by using a riding model (SHELXL-97).^[30]

CCDC-633570 contains the supplementary crystallographic data for this paper. These data can be obtained free of charge from The Cambridge Crystallographic Data Centre via www.ccdc.cam.ac.uk/data_request/cif.

Supporting Information (see footnote on the first page of this article): Positive ESI⁺-MS spectrum of Pd₂(L)₂·2MeCN·6H₂O and summary of the face-to-face and edge-to-face interactions found in the crystal structures of Cu₂(L)₂·2MeCN and H₂L.

Acknowledgments

The authors are grateful to Xunta de Galicia (PGID-IT06PXIB209043PR) for financial support.

- [1] D. Gatteschi, O. Kahn, J. S. Millar, F. Palacio in *Magnetic Molecular Materials*, Kluwer Academic, Dordrecht, **1991**.
- [2] O. Kahn in *Molecular Magnetism*, VCH Publishers, New York, **1993**.
- [3] R. E. P. Winpenny, *Chem. Soc. Rev.* **1998**, 27, 447.
- [4] H. Hu, D. Zhang, Z. Chen, C. Liu, *Chem. Phys. Lett.* **2000**, 329, 255.
- [5] C. Benelli, D. Gatteschi, *Chem. Rev.* **2002**, 102, 2369.
- [6] J.-P. Costes, F. Dahan, J. García-Tojal, *Chem. Eur. J.* **2002**, 8, 5430.
- [7] A. K. Bondalis, J. Clemente, M. Juan, F. Dahan, *Inorg. Chem.* **2004**, 43, 1574.
- [8] M. Fondo, N. Ocampo, A. M. García-Deibe, M. Corbella, M. R. Bermejo, J. Sanmartín, *Dalton Trans.* **2005**, 3785–3794.
- [9] A. I. Uraev, I. S. Vasilchenko, V. N. Ikorskii, T. A. Shestakova, A. S. Burlov, K. A. Lyssenko, V. G. Vlasenko, T. A. Kuz'menko, L. N. Divaeva, I. V. Pirog, G. S. Borodkin, I. E. Uflyand, M. Y. Antipin, V. I. Ovrachenko, A. D. Garnovskii, V. I. Minkin, *Mendeleev Commun.* **2005**, 133–135.
- [10] M. Bernal, J. A. García-Vázquez, J. Romero, C. Gómez, M. L. Durán, A. Sousa, A. Sousa-Pedrares, D. J. Rose, K. P. Maresca, J. Zubietta, *Inorg. Chim. Acta* **1999**, 25, 39–47.
- [11] A. D. Garnovskii, A. S. Burlov, D. A. Garnovskii, I. S. Vasilchenko, A. S. Antsichkina, G. G. Sadikov, A. Sousa, J. A. García-Vázquez, J. Romero, M. L. Durán, A. Sousa-Pedrares, C. Gómez, *Polyhedron* **1999**, 18, 863–869.
- [12] B. I. Kharisov, D. A. Garnovskii, M. L. Blanco, A. S. Burlov, I. S. Vasilchenko, A. D. Garnovskii, *Polyhedron* **1999**, 18, 985–988.
- [13] D. A. Garnovskii, M. F. C. Guedes da Silva, M. N. Koplovich, A. D. Garnovskii, J. J. R. Frausto da Silva, A. J. L. Pombeiro, *Polyhedron* **2003**, 22, 1335–1340.
- [14] a) F. H. Allen, *Acta Crystallogr., Sect. B* **2002**, 58, 380; b) I. J. Bruno, J. C. Cole, P. R. Edginton, M. Kessler, C. F. Macrae, P. McCabe, J. Pearson, R. Taylor, *Acta Crystallogr., Sect. B* **2002**, 58, 389.
- [15] M. R. Churchill, F. J. Hollander, J. R. Shapley, J. B. Keister, *Inorg. Chem.* **1980**, 19, 1272–1277.
- [16] See for example: a) H. Fuess, J. W. Bats, M. Diehl, L. Schonfelder, H. W. Roesky, *Chem. Ber.* **1981**, 114, 2369; b) H. Puff, D. Hanssger, N. Beckermann, A. Roloff, W. Schuh, *J. Organomet. Chem.* **1989**, 373, 37; c) G. Besenyei, L. Parkanyi, I. Foch, L. I. Simandi, A. Kalman, *Chem. Commun.* **1997**, 1143; d) I. Foch, L. Parkanyi, G. Besenyei, L. I. Simandi, A. Kalman, *J. Chem. Soc., Dalton Trans.* **1999**, 293–299; e) G. Besenyei, L. Párkányi, I. Foch, L. Simándi, *Angew. Chem. Int. Ed.* **2000**, 39, 956–958; f) R. T. Ruck, R. G. Bergman, *Organometallics* **2004**, 23, 2231–2233.
- [17] S. Ali, A. J. Deeming, G. Hogarth, N. A. Mehta, J. W. Steed, *Chem. Commun.* **1999**, 2541–2542.
- [18] L. Menabue, M. Saladini, *Inorg. Chem.* **1991**, 30, 1651–1655.
- [19] J. Sanmartín, F. Novio, A. M. García-Deibe, M. Fondo, M. R. Bermejo, *New J. Chem.* **2007**, 31, 1605.
- [20] a) H.-Y. Cheng, P.-H. Cheng, C.-F. Lee, S.-M. Peng, *Inorg. Chim. Acta* **1991**, 181, 145–147; b) C. A. Otter, S. M. Couchman, J. C. Jeffery, K. L. V. Mann, E. Psillakis, M. D. Ward, *Inorg. Chim. Acta* **1998**, 278, 178–184; c) S. Cabaleiro, P. Perez-Lourido, J. Castro, J. Romero, J. A. García-Vázquez, A. Sousa, *Transition Met. Chem.* **2001**, 26, 709–716; d) A. Sousa, M. R. Bermejo, M. Fondo, A. M. García-Deibe, A. Sousa-Pedrares, O. Piro, *New J. Chem.* **2001**, 25, 647–654; e) M. E. Bluhm, M. Ciesielski, H. Görls, O. Walter, M. Döring, *Inorg. Chem.* **2003**, 42, 8878–8885.

- [21] a) N. C. Baenziger, A. S. Struss, *Inorg. Chem.* **1976**, *15*, 1807–1809; b) S. Cabaleiro, J. Castro, E. Vázquez-López, J. A. García-Vázquez, J. Romero, A. Sousa, *Inorg. Chim. Acta* **1999**, *294*, 87–94; c) J. Sanmartín, A. M. García-Deibe, M. R. Bermejo, F. Novio, D. Navarro, M. Fondo, *Eur. J. Inorg. Chem.* **2003**, 3905–3913; d) I. Beloso, J. Castro, J. A. García-Vázquez, P. Pérez-Lourido, J. Romero, A. Sousa, *Inorg. Chem.* **2005**, *44*, 336–351.
- [22] a) O. I. Singh, M. Damayanti, N. R. Singh, R. K. H. Singh, M. Mohapatra, R. M. Kadam, *Polyhedron* **2005**, *24*, 909–916; b) S. P. Devi, R. K. H. Singh, R. M. Kadam, *Inorg. Chem.* **2006**, *45*, 2193–2198; c) L. A. Sharma, O. I. Singh, A. M. Singh, R. K. H. Singh, R. M. Kadam, M. K. Bhide, A. R. Dhobale, M. D. Sastry, *Spectrochim. Acta, Part A* **2004**, *60*, 1593–1600.
- [23] N. Sreehari, P. T. Manoharan, *Mol. Phys.* **1988**, *63*, 1077–1093.
- [24] B. Bleaney, K. D. Bowers, *Proc. R. Soc. London, Ser. A* **1952**, *214*, 451–465.
- [25] E. Ruiz, J. Cano, S. Álvarez, P. Alemany, *J. Am. Chem. Soc.* **1998**, *120*, 11122–11129.
- [26] C. Mealli, D. M. Proserpio, *J. Chem. Educ.* **1990**, *67*, 399–402.
- [27] H. Chowdhury, S. H. Rahaman, R. Ghosh, S. K. Sarkar, M. Corbella, B. K. Ghosh, *Inorg. Chem. Commun.* **2006**, *9*, 1276–1280.
- [28] M. Fondo, A. M. García-Deibe, M. Corbella, J. Ribas, A. Llamas-Saiz, M. R. Bermejo, J. Sanmartín, *Dalton Trans.* **2004**, 3503–3507.
- [29] a) T. Adatia, N. Beynek, B. P. Murphy, *Polyhedron* **1995**, *14*, 335–338; b) D. Zurita, P. Baret, J.-L. Pierre, *New J. Chem.* **1994**, *18*, 1143–1146; c) G. Mugesh, H. B. Singh, R. P. Patel, R. J. Butcher, *Inorg. Chem.* **1998**, *37*, 2663–2669; d) G. Mugesh, H. B. Singh, R. J. Butcher, *Eur. J. Inorg. Chem.* **1999**, 1229–1236.
- [30] G. M. Sheldrick, *SHELXL-97, Program for the Refinement of Crystal Structure*, University of Göttingen, Germany, **1998**.

Received: December 14, 2007

Published Online: February 19, 2008